Lipids as therapeutic targets for barrier repair in skin diseases

Boiten, W.A.

Part III

Chapter 6

Selectivity in cornified envelop binding of ceramides in human skin and the role of LXR inactivation on ceramide binding

Authors and affiliations:

W.A. Boiten[a], R.W.J. Helder[a], J. van Smeden[a,b], J.A. Bouwstra[a]

[a]Department of Drug Delivery Technology, Cluster BioTherapeutics, Leiden Academic Centre for Drug Research, Leiden University, Leiden, the Netherlands

[b]Current address: Centre for Human Drug Research, Leiden, The Netherlands.

Published as and adapted from:
Biochim Biophys Acta Mol Cell Biol Lipids. 2019 Sep;1864(9):1206-1213.

Background:
Spectra of the bound ceramides and their unbound conterparts (left bound OS, rigth unbound EOS)

6 Selectivity in cornified envelope binding of ceramides

Abstract

The cornified lipid envelope (CLE) is a lipid monolayer covalently bound to the outside of corneocytes and is part of the stratum corneum (SC). The CLE is suggested to act as a scaffold for the unbound SC lipids. By profiling the bound CLE ceramides, a new subclass was discovered and identified as an omega-hydroxylated dihydrosphingosine (OdS) ceramide. Bound glucosylceramides were observed in superficial SC layers of healthy human skin. To investigate the relation between bound and unbound SC ceramides, the composition of both fractions was analyzed and compared. Selectivity in ceramide binding towards unsaturated ceramides and ceramides with a shorter chain length was observed. The selectivity in ceramide species bound to the cornified envelope is thought to have a physiological function in corneocyte flexibility. Next, it was examined if skin models exhibit an altered bound ceramide composition and if the composition was dependent on liver X-receptor (LXR) activation. The effects of an LXR agonist and antagonist on the bound ceramides composition of a full thickness model (FTM) were analyzed. In FTMs, a decreased amount of bound ceramides was observed compared to native human skin. Furthermore, FTMs had a bound ceramide fraction which consisted mostly of unsaturated and shorter ceramides. The LXR antagonist had a normalizing effect on the FTM bound ceramide composition. The agonist exhibited minimal effects. We show that ceramide binding is a selective process, yet, still is contingent on lipid synthesized.

KEYWORDS:
cornified lipid envelope, bound lipids, ceramide, quantification, skin culture, liver-X-receptor.

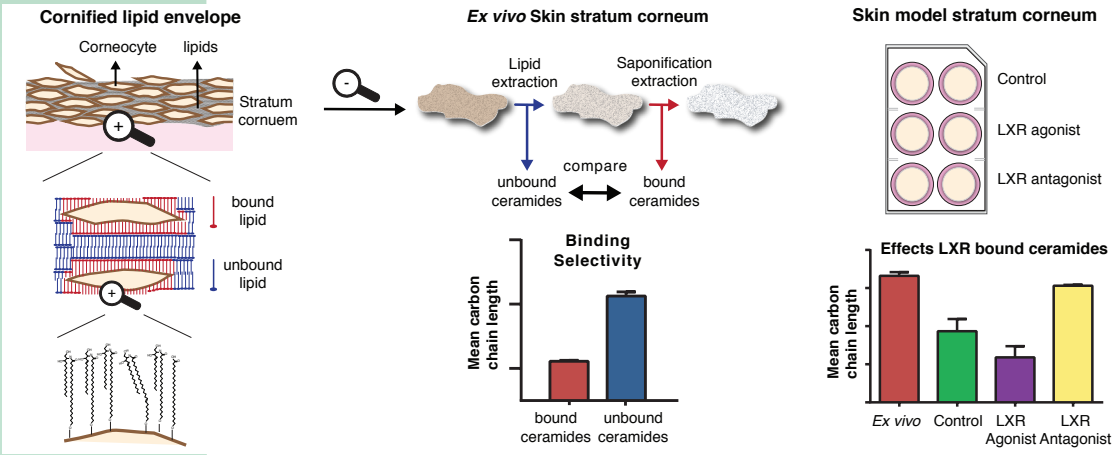

Graphical abstract

6.1 Introduction

The outer skin layer, the stratum corneum (SC), consists mainly of terminally differentiated keratinocytes (corneocytes) embedded in an extracellular lipid matrix of ceramides, free fatty acids, and sterols. During the terminal differentiation process, the plasma membrane is replaced by a crosslinked protein structure called the cornified envelope (CE)[1]. Covalently bound to the CE is a monolayer of lipids referred to as the cornified lipid envelope (CLE). These lipids act as an interface between the hydrophilic corneocytes and the lipophilic extracellular lipids and are therefore an essential part of the skin barrier[2,3]. With a reduced CLE mice exhibit severe skin barrier problems[4].

It has been reported that the CLE consists of ceramides and fatty acids[5-7]. Ceramides are composed of two parts: a sphingoid base and an acyl chain. The molecular architecture of the ceramide its hydrophilic head group defines the ceramide subclass[8]. The bound ceramides comprise of a subset of the unbound subclasses[5,6], **Supplemental S6.1** depicts the structures of these subclasses. This subset has an omega-hydroxylated acyl chain (OCers). The hydroxylated group at the end of the carbon tail facilitates an ester linkage to the CE proteins[9,10]. It also facilitates the binding of a linoleic acid. Both unbound SC ceramides (in the lipid matrix) and the bound SC ceramides (attached to cornified envelope) originate from the same pool of precursor lipids[11].

During the differentiation process the SC lipids are synthesized by keratinocytes[12]. In the upper part of the viable epidermis keratinocytes contain specific lipid vesicles called lamellar bodies. They contain the bound and unbound precursor lipids. At the interface between the viable epidermis and SC, ceramide precursors (glycosylated (GlcCers) or phosphocholinated (sphingomyelin) ceramides[13]) are released into the extracellular space together with the enzymes to convert them[14]. Simultaneously, formation of the CLE occurs[15,16]. Enzymes involved in ceramide binding to the CE have been colocated at the viable epidermis SC interface[17]. Essential to ceramide binding is that ceramides have I) a linoleate esterified omega-hydroxylated acyl chain (EOCers)[18-20] and II) are glycosylated. The esterified linoleate is removed, the GlcCers are bound, and thereafter, they are cleaved to ceramides[11]. Which ceramides of the pool of precursors are bound and if this is a selective process is not yet reported.

To study which ceramides are selected for CE binding, SC from *ex vivo* skin and from skin models was used. Comparing the composition of both bound and unbound lipid extracts of *ex vivo* SC could elucidate whether ceramide binding is a selective process. Human skin equivalent full thickness models (FTMs) were selected as skin model. These models mimic aspects of normal human skin including SC generation. Yet, in FTMs the SC lipids had an increased fraction of unsaturated ceramides and a reduced mean ceramide chain length[21,22]. It was hypothesized that the bound lipid fraction of FTMs was altered too. LXR is a nuclear receptor sensitive for sterols and responsible for

multiple lipid processing pathways[23], one of which is regulation of Stearoyl coenzyme A desaturase 1, responsible for the desaturation of fatty acids also used in the epidermal ceramide biosynthesis[24]. By adding a liver X-receptor (LXR) agonist or antagonist, the lipid metabolism of FTMs can be manipulated[25]. LXR signaling was hypothesized to affect the bound lipids in FTMs as well.

Recently, a new LC-MS method to simultaneously profile and quantify the unbound SC ceramide fraction was developed and could be applied to discover new bound ceramides[26]. Quantification of the entire bound ceramide profile provides insight into subclass and chain length distribution and the degree of unsaturation. This method was applied to the bound ceramide fractions of *ex vivo SC*, tape stripped SC, and FTMs. We aimed to examine if ceramide binding is a selective process and if this process is affected in FTM by an LXR agonist or antagonist.

6.2 Materials and Methods

6.2.1 Chemicals

For extraction and analysis of the lipids the following solvents were used: UPLC grade methanol, ethanol, iso-propanol (Biosolve, Valkenswaard, the Netherlands), HPLC grade methanol, chloroform (Lab-Scan Gliwice, Poland), and n-heptane, and milli-Q water (18.2Ω). KCL and NaOH (Merck KGaA, Darmstadt, Germany) were used in the extraction. **Supplemental S6.2** contains a list of standards and the internal standard used for ceramide quantification.

6.2.2 Samples

All human skin was obtained after institutional approval and a written informed consent according the declaration of Helsinki.

6.2.2.1 Ex vivo SC samples

Skin from two mammoplasties and one abdominoplasty was dermatomed to a thickness of 0.6 mm within 24 hours after surgery. The dermatomed skin was incubated overnight on filter paper containing 0.1% trypsin solution in PBS and thereafter digested for 1 hour at 37°C. SC sheets were peeled off, thoroughly washed with 0.1% trypsin-inhibitor followed by 2x milli-Q water, and were air dried before storage. For each donor, 3 SC samples of each ~3.5 mg SC dry weight were used for lipid extraction and subsequent bound lipid extraction.

6.2.2.2 In vivo tape-stripped SC samples

One site on the ventral forearm of the volunteer was tape-stripped using polyphenylene sulfide tape (Nichiban, Tokyo, Japan). Equal pressure was applied on the tapes using a 1 kg weight and a D-squame pressure instrument with additional foam pad and the removal direction alternated. The amount of material on the tapes was determined by detecting the absorption at 850nm using a SquameScan (Heiland Electronic, Wetzlar, Germany), subtracting the absorbance of a blank tape. The first five tapes were discarded and four consecutive tapes were used for the bound lipid extraction. Each tape was extracted individually.

6.2.2.3 Full thickness models SC samples

FTMs were generated using isolated human keratinocytes obtained from three different skin donors. Keratinocytes were seeded on a collagen gel populated with fibroblasts and FTMs were generated as described by Thakoersing et al.[22]. LXR activation or inhibition was induced by supplementation of the agonist T0901317 or antagonist GSK2033, respectively (Sigma Aldrich, Zwijndrecht, the Netherlands). The concentration of the agonist and antagonist in the medium was 500 nM (with an EC_{50} of 50nM and IC_{50} of 32nM, respectivaly); 0.05 vol% of a 1mM stock in DMSO. For each donor FTMs were generated under four different conditions: $FTM_{CONTROL}$ (normal medium), FTM_{DMSO} (medium + DMSO), $FTM_{AGONIST}$ (Medium + Agonist), and $FTM_{ANTAGONIST}$ (Medium + Antagonist). The FTMs SC was isolated as described above.

6.2.3 Lipid extractions

The SC samples were dried under vacuum at 50°C, stored under N_2, and weighted using a microbalance ME5 (Sartorius, Bradford, MA, USA). To obtain the unbound lipids, SC sheets and tape-strips were first extracted using a modified four step Bligh and Dyer procedure[26]. MilliQ and 0.04 vol% of aqueous 0.25M KCl was added to the combined extracts of the four steps. After phase separation over night at 4°C the organic layer was collected. Thereafter, the hydrophilic layer was washed with chloroform and the organic layers were combined, filtered (0.20µM PTFE filter), evaporated under N_2, and reconstituted in chloroform:methanol (2:1, v:v), 0.4 ml per mg SC dry weight.

After extraction of the unbound lipids, the SC sheets were washed with chloroform and dried under vacuum. A solution of 10% 1M aqueous NaOH and 90% methanol (v:v) was added to the dried samples to detach the bound lipids. For saponification the samples were shaken for 1 hour with 120 rpm at 60°C. To stop the reaction, the pH of the samples was decreased to a final pH between 4-7 using 1M and 0.1M HCl. After saponification tape-strips and SC sheets were further extracted at 40°C

by using subsequently: chloroform:methanol (1:1, v:v), chloroform:methanol (2:1, v:v), and heptane:Isopropanol (1:1, v:v). Thereafter, the combined bound lipid extracts were treated as described above for the unbound lipids. The extraction efficiency and recovery of the bound lipid extraction are described in **Supplemental S6.3** and were both above 90%.

Before analysis, the concentration of the unbound and bound lipids extracts was determined by the gravimetrical difference of a specific volume before and after drying. For LC-MS analysis, unbound lipid samples were prepared at 0.3 mg/ml of extract and tape-strip extract at 20 tapes/ml. Bound lipids samples were prepared at 0.1 mg/ml and tape-strip extracts at 40 tapes/ml. All samples were dissolved in heptane:chloroform:methanol (95:2.5:2.5, v:v:v) with internal standard added at 0.6 µM.

6.2.4 LC-MS and LC-MS/MS analysis

All samples were analyzed and quantified using a Waters Acquity UPLC H-class (Waters, Milford, MA, USA) connected to an XEVO TQ-S mass spectrometer (Waters, Milford, MA, USA). Of the samples, 5 µl was injected and separated on a pva-silica column (5 µM particles, 100x2.1mm i.d.)(YMC, Kyoto, Japan). Quantitative analysis was performed as described previously[26]. For identification, LC-MS/MS data were obtained with Scanwave daughter scan mode on the m/z values of interest with fragmentation energies of 40 or 50 eV. **Supplemental S6.4** shows the m/z ratios analyzed to identify the omega-hydroxylated dihydrosphingosine (OdS) ceramide.

6.2.5 Quantification

All ceramides that were identified in the bound and unbound fraction of the *ex vivo* SC samples were quantified to pmol and ng injected into the LC. Because the bound lipid extracts contained other materials than lipids (explained below), it was essential to normalize it to SC dry weight. The total amount of material extracted from the SC was calculated by multiplying the concentration of the extract with the volume in which it was dissolved. Either 1.5 µg (unbound sample) or 0.5 µg (bound sample) of this material was injected into the LC. The total amount of ceramides detected in this injected fraction of the sample was used to calculate the amount of ceramides in the complete extract (nmol or µg). The total amount of ceramides in the extract (µg) was normalized to the SC dry weight in mg. To determine which fraction of ceramides was bound, molar amounts per mg of SC of the unbound and bound ceramides were compared.

As a control for the gravimetrical approach to determine the bound lipid

amount extracted, three blank saponified extractions were performed. **Supplemental S6.5** shows the results and discussion of these experiments. It was concluded that in saponified extracts excess non-lipid materials (most probably salts) were present.

6.2.6 Software and statistics

LC-MS and LC-MS/MS data analysis was performed using MassLynx and TargetLynx V4.1 SCN 843 (Water Inc. Milford, MA, USA). Statistical analyses were performed using linear mixed modeling in SPSS version 24 (IBM Corp.). A detailed description of the models is given with the corresponding Supplemental.

6.3 Results

6.3.1 Profiling and quantification

To examine which bound ceramides could be detected by our method, a profile was made by LC-MS. **Figure 6.1A** depicts an ion-map profile of a 0.5 µg *ex vivo* SC bound ceramide extract. Previously observed ceramide subclasses OS, OP, and OH were detected, however, additional compounds were detected as well. The retention times (Rts) of two groups of compounds corresponded to the Rts of GlcCers and had masses corresponding to Glc-OS and Glc-OH subclasses. A part of the GlcCers loses their glucose group during ionization. This was used to confirm the presence of bound GlcCers by detecting OS at the same Rt as Glc-OS (**Supplemental S6.6**). Bound GlcCers were also detected in a tape-strip sample, yet, they are not observed in the corresponding unbound fraction.

One group of compounds had a shorter Rt than that of subclass OS and a mass of 2 amu higher. To confirm that this was the suspected subclass OdS, fragmentation of 3 saturated, 2 unsaturated, and 1 odd number chain length of these compounds was performed (**Supplemental S6.4**). **Figure 6.1B** depicts the fragmentation spectrum of OdS C52:0. The characteristic fragments of dS ceramides were observed (294.3 and 322.3 amu). As comparison a fragmentation spectrum of OS C52:0 is shown in **Figure 6.1C**, depicting a sphingoid fragment two amu lower (292.3 and 320.3 amu). Finally, a group of compounds was observed with the mass of an omega-hydroxyl acyl chain with a dihydroxy-dihydrosphingosine (T). The latter was described by t' kind et al[27]. Combined with their long Rt we assumed this is ceramide subclass OT. Only including the subclasses OdS, OS, OP and OH, a total of 103 different bound ceramides were detected in *ex vivo* SC bound lipid extracts.

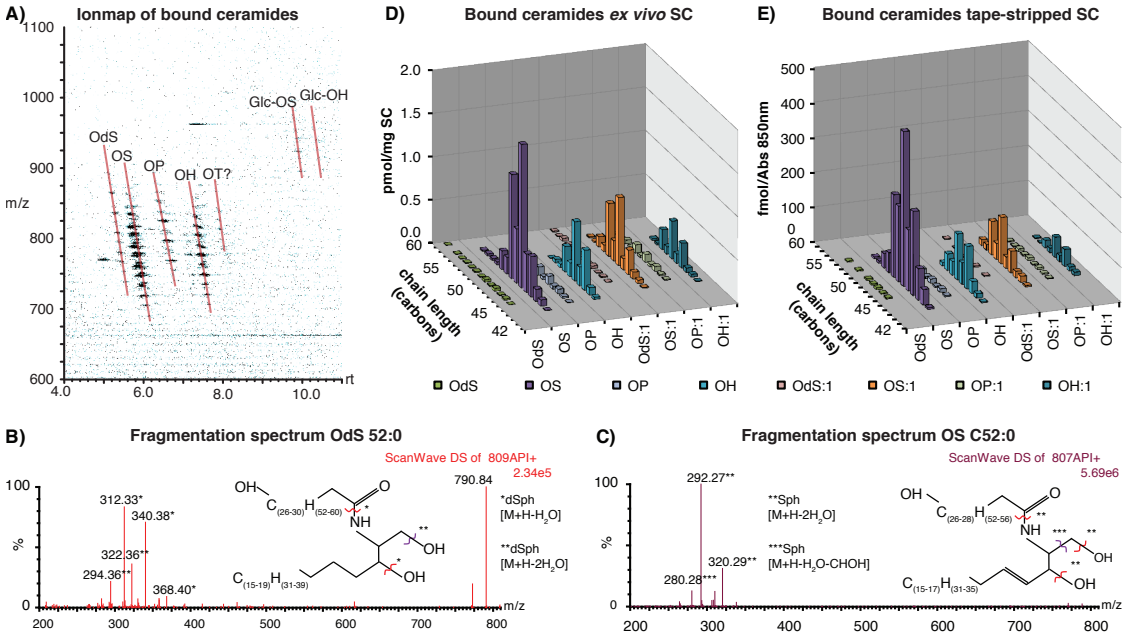

Figure 6.1: Profiling of bound ceramide fraction

A: *An ion-map of the bound ceramide fraction of ex vivo SC. Each ceramide subclass is indicated by a red line.* ***B:*** *Fragmentations spectrum of the compound eluting before OS, m/z 808.81 and collision energy of 40eV.* ***C:*** *Fragmentations spectrum of OS C52:0, m/z 806.80 and collision energy of 50eV.* ***D and E:*** *The amount of all quantified bound ceramides shown per subclass and chain length of an ex vivo SC samples and a tape-stripped SC sample, respectively.*

Thereafter, the profiled bound ceramides were quantified. Next to *ex vivo* SC, a tape strip extract was examined to determine if this method was applicable to this sample type. **Figure 6.1D and E** show the quantitative profiles of a representative *ex vivo* SC sample and a tape-strip sample, expressed as the molar ceramide amount per mg SC or the amount per amount SC stripped (expressed as absorbance at 850nm), respectively. The profile showed that: 1) It is possible to isolate the bound ceramides from tape-stripped SC after extraction of the unbound ceramides; 2) the bound ceramide profile of a tape-strip sample was similar to that of an *ex vivo* SC sample.

To compare the bound and unbound fractions, the total amount of unbound ceramides in the *ex vivo* SC was quantified. Unbound and bound ceramide amounts are provided in **Figure 6.2**. **Figure 6.2A** depicts the total unbound and bound ceramide amounts in µg per mg SC, whereas **Figure 6.2B** depicts the molar percentage of ceramides that were bound. It was observed that: I) there were no large differences between the bound ceramide amounts of the three donors; II) 2.5-4 w% of the SC weight was ceramides; and III) about 20 mol% of the ceramides in the SC was bound.

Table 6.1 depicts the relative molar amount (%) of each bound ceramide subclass to the total bound ceramides amount. In the next section, the bound ceramide fraction and how it relates to the unbound fraction will be examined in more detail.

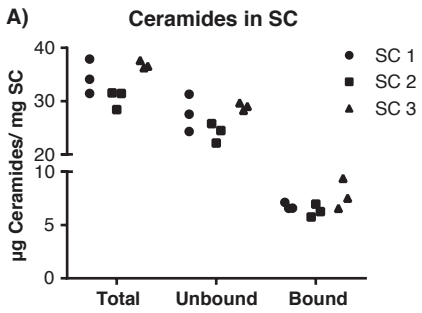

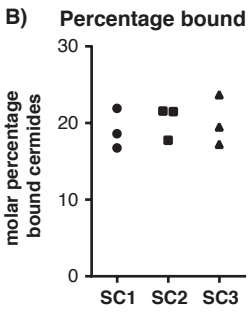

Figure 6.2: Ceramide fraction of the SC

A: *The amount of ceramides in ex vivo SC as µg of ceramides per mg of SC.* **B:** *The percentage of ceramides which was bound for the three SC donors (SC1, 2 and 3).*

Table 6.1: *The relative molar amounts of the bound ceramides per subclass. Given as the mean and SD (n=3). The ∑ molar amount of all bound ceramides in a sample was set to 100%.*

	SC 1		SC 2		SC 3	
Subclass	Molar %	SD	Molar %	SD	Molar %	SD
OdS	1.5	>0.1	2.3	0.3	1.3	>0.1
OS	51.1	0.5	48.6	0.7	43.9	1.3
OP	3.8	0.3	5.1	0.2	3.5	0.1
OH	20.6	0.2	25.3	0.7	17.7	1.0
OdS:1	0.8	0.1	0.9	0.2	1.4	0.3
OS:1	13.3	0.2	9.3	0.1	18.8	1.5
OP:1	2.1	>0.1	2.1	0.2	3.1	0.2
OH:1	6.8	0.3	6.3	0.1	10.3	0.3

6.3.2 Selectivity in ceramide binding

To examine if there is selectivity in ceramide binding, the differences in composition between the bound and unbound ceramide fraction of *ex vivo* SC were determined. It was observed that the bound ceramides contained large amounts of ceramides with a monounsaturated acyl chain (MuCers) and this was higher than the unbound fraction (**Figure 6.3A**). Differences in MuCer % between the 3 donors were observed. Changes for each donor were consistent; if the unbound MuCer% increased, the bound MuCer% increased too. MS/MS fragmentation of the MuCers showed that the double bond was only present in the ceramides acyl chain (**Supplemental S6.7**).

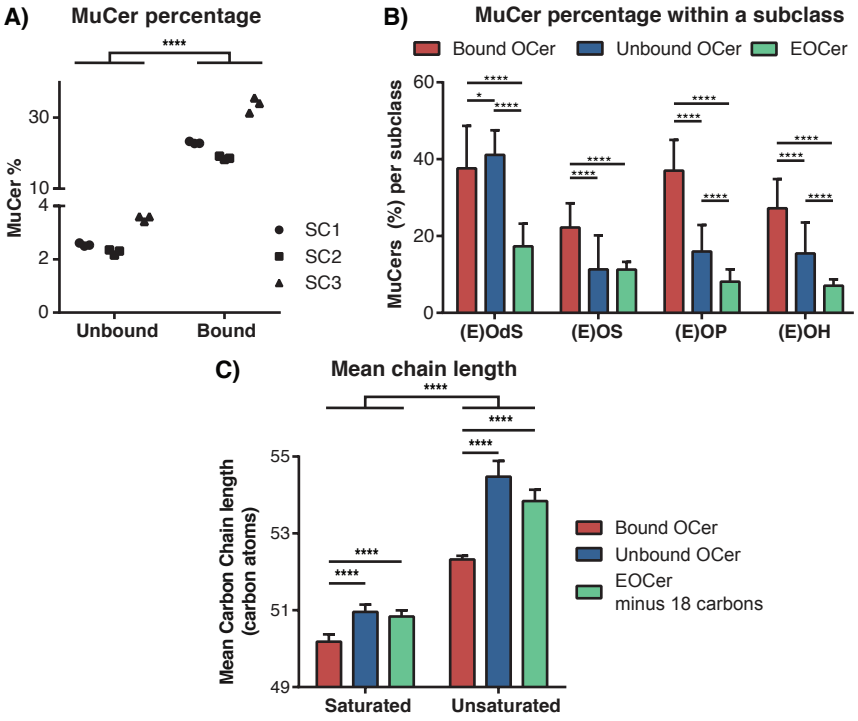

Figure 6.3: Selectivity in ceramide binding for multiple parameters

A: *The percentage of MuCers in the bound and unbound ceramides of three SC donors.* ***B:*** *The percentage of MuCers within a subclass, comparing the bound OCer, unbound OCer, and EOCer with the same sphingoid base. In a sample, the sum of both the saturated and unsaturated ceramides of a subclass was set as a 100%.* ***C:*** *The MCL of the bound and unbound OCers is shown for the saturated and unsaturated ceramides. From the EOCers MCL, 18 carbons were subtracted to compensate for the linoleate moiety. Bars are mean ±SD of 9 samples, 3 per donor. Parameter estimates of the fixed effects are given in* ***supplemental S6.8 and S6.9****.*

To compare the bound and unbound ceramides originating from the same GlcCers, the unbound counterparts of the bound ceramides fraction were examined: EOCers and OCers. The unbound ceramides with the highest MuCers content were the EOCer and OCer subclasses (**Supplemental S6.8**). Of the bound and unbound ceramides the MuCers percentage within each subclass was determined and plotted per subclass (**Figure 6.3B**). Comparing these data with a linear mixed model showed that the bound OCer fraction consisted of a significantly higher MuCers percentage than both the unbound EOCer and OCer subclasses, except for subclass OdS (**Supplemental S6.9** depicts the linear mixed model results). In the unbound fraction, subclasses OdS, OP, and OH contained a higher percentage MuCers than their corresponding EOCer subclasses. Comparing the bound and unbound ceramides degree of unsaturation indicates selective binding towards unsaturated ceramides.

Alongside the MuCers percentage, the bound and unbound fractions mean carbon chain lengths (MCL) were calculated. To compare the bound and unbound subclasses, the MCL of the OCer and EOCer subclasses were determined. MuCers are depicted separately because they had a longer MCL than saturated ceramides (linear mixed model results **Supplemental S6.10**). To compare the EOCer to the OCer, 18 carbons were subtracted from EOCers MCL to compensate for the esterified linoleates additional 18 carbons. **Figure 6.3C** depicts the MCL for the bound OCer, unbound OCer, and unbound EOCer. The MCL of the bound ceramides differed significantly from that of the unbound ceramides. For both the saturated ceramides and MuCers, the MCL was shorter in the bound lipid fraction. The chain length of both unbound OCers and the EOCer-C18 were comparable. These findings on MCL show that there was selectivity toward binding of shorter ceramides to the cornified envelope.

6.3.3 The effect of LXR on the bound lipid fraction in FTMs

Previously, alterations in unbound SC ceramides of FTMs were observed. It was examined if similar changes were observed in the bound ceramide fraction and if the bound ceramides were influenced by the LXR. In **Figure 6.4A** quantitative amounts of bound ceramides/mg SC are provided for four FTM conditions: $FTM_{CONTROL}$, FTM_{DMSO}, $FTM_{AGONIST}$, and $FTM_{ANTAGONIST}$. No differences in the total amount of bound ceramides were observed between the various FTM conditions. It was observed that there was a significantly lower quantity of bound ceramides in the FTMs compared to *ex vivo* SC samples. **Supplemental S6.11** gives an overview of the statistical tests and output comparing the sample groups. **Supplemental S6.11** depicts that in FTMs an oleate was attached to the EOCers instead of a linoleate.

When examining the bound lipid fraction of the FTMs, it consisted predominantly of MuCers (**Figure 6.4B**) and even polyunsaturated ceramides (PuCer) were detected. **Table 6.2** depicts the relative molar composition of the four different conditions. The percentage of bound MuCers in FTMs was significantly higher than in *ex vivo* SC. By adding an LXR antagonist a significant decrease in the percentage of MuCers was observed. No effect was observed from adding the LXR agonist.

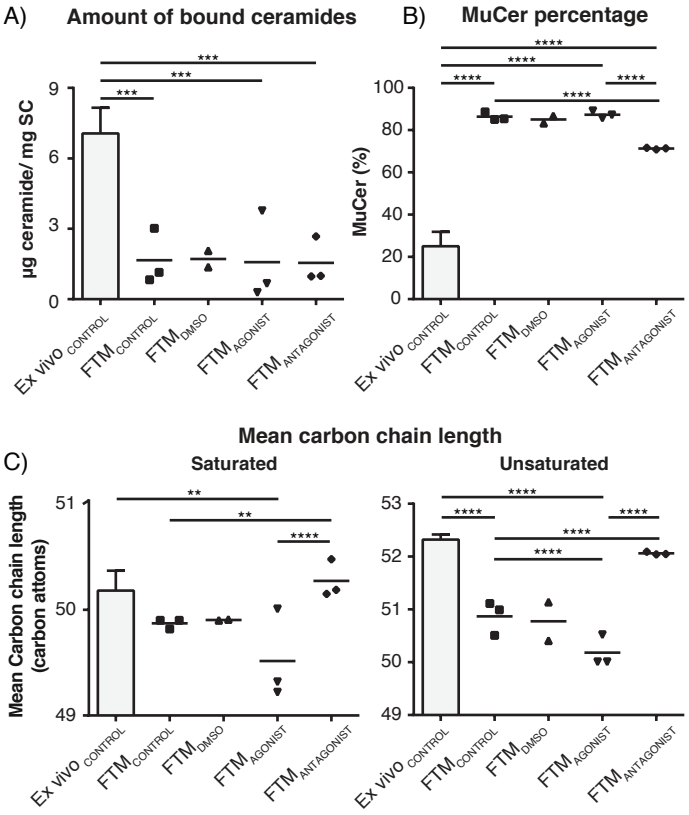

Figure 6.4: Effects of LXR in FTMs on the bound lipids

A: The amount of bound ceramides per mg SC. B: The percentage of the bound ceramides that had a monounsaturated acyl chain. C: The MCL of the saturated and unsaturated ceramides. All depict the ex vivo control as bar (mean +SD n=9), FTMs: CONTROL, DMSO, AGONIST and ANTAGONIST, are shown as individual points and mean. Parameter estimates of the fixed effects are given in ***Supplemental S6.10.***

For FTMs the bound ceramides MCL of saturated and unsaturated bound ceramides was determined and compared to that of *ex vivo* SC (**Figure 6.4C**). In FTMs, a significant decreased MuCers MCL was observed compared to *ex vivo* SC. The MCL was further decreased by the LXR agonist. However, using the LXR antagonist the MCL is increased to the MCL of *ex vivo* SC. Due to the lower percentages of saturated ceramides (see **Table 6.2**), the MCL of the saturated ceramides was predominantly based on subclass OS. Nonetheless, the same trends were observed as in the MuCers. Concluding, FTMs had an altered bound lipid composition compared to *ex vivo* SC. An LXR antagonist had a normalizing effect on the FTMs bound ceramide composition, reducing the percentage of MuCers and increasing the MCL.

Table 6.2: *The mean and SD (n=3 except DMSO which had n=2) of the bound lipids relative molar subclass amount in FTMs. For each sample the ∑ molar amount of all bound ceramides was set to 100%.*

	$FTM_{CONTROL}$		FTM_{DMSO}		$FTM_{AGONIST}$		$FTM_{ANTAGONIST}$	
subclass	Molar %	SD	Molar %	SD	Molar %	SD	Molar %	SD
OdS	n.d*		0.4	n.a.**	0.6	n.a.**	0.6	0.4
OS	6.8	1.4	6.5	1.1	3.4	1.1	17.5	1.8
OP	0.6	n.a.**	0.8	n.a.**	0.5	0.2	0.9	0.6
OH	2.9	0.6	2.9	0.4	2.8	0.6	8.0	0.2
OdS:1	2.4	0.7	3.5	2.0	3.2	0.2	2.7	0.5
OS:1	53.4	1.2	52.2	3.4	51.6	4.3	42.8	1.2
OP:1	6.2	0.9	6.6	1.7	7.5	0.8	6.1	0.6
OH:1	24.4	3.4	22.7	2.6	25.1	4.3	19.7	2.0
OdS:2	0.3	n.a.**	0.9	n.a.**	0.9	0.0	0.2	n.a.**
OS:2	2.5	0.2	3.1	0.4	3.5	0.1	1.6	1.0
OP:2	0.3	n.a.**	0.2	n.a.**	0.5	n.a.**	0.1	n.a.**
OH:2	1.0	0.3	1.2	0.3	1.8	0.4	0.9	n.a.**

*n.d. not detected

**n.a. not available (only detected in one of the replicates)

6.4 Discussion

Selectivity in ceramide cornified envelope binding was observed by comparing compositions of the unbound EOCer and OCer subclasses to the bound SC ceramide fractions. In FTMs, the ceramide binding was reduced and the bound ceramide composition influenced by LXR. The new ceramide subclass OdS was identified[5-7]. Furthermore, a ceramide subclass with masses corresponding to an omega-hydroxy acyl dihydroxy-dihydrosphingosine (OT) was observed. It was hypothesized that dihydroxy-dihydrosphingosine exists as a bound ceramide, because these sphingoid bases have been observed attached to the various acyl chains of the unbound lipids (unpublished data).

Using the compositional differences between the bound and unbound ceramides, it was shown that bound ceramides had a higher degree of unsaturation and shorter carbon chains than their unbound counterparts. Both the bound and unbound ceramides are thought to originate from the same pool of precursor GlcCers[28]. Thus, during the binding process there was selectivity towards MuCers and shorter chain ceramides. Selectivity in ceramide binding conceivably has a physiological importance to provide corneocyte flexibility. Bound lipids form a template for the formation of the SC lipid organization and can align the lipid lamellae parallel to the cornified

envelope[4,29,30]. Furthermore, the SC and within it the corneocytes, are not rigid structures but require flexibility[31-33]. Atomic force microscopy studies showed that the CLE is less rigid than the internal corneocyte structures[31,32]. With different hydration states the shape of corneocyte changes[33], requiring flexibility which should also be provided by the CLE. Flexibility of the CLE might be enhanced by a shorter MCL[34,35] and the presence of MuCers, although it is unknown if these are cis or trans configured either would impact the flexibility.

In FTMs, a lower amount of bound ceramides per mg dry SC was observed than in *ex vivo* SC. Previously published results showed no reduction[36]. It is likely that the observed reduction is due to the reduction of a precursor in the ceramide binding pathway (**Figure 6.5**). In the unbound ceramides of FTMs a large fraction of EOCers contained an esterified oleic acid (**Supplemental S6.12**)[37]. Previously, it has been shown that at the viable epidermis SC interface the linoleic acid is converted to an epoxide by 12R-LOX and subsequently to a hydroxy-epoxide by e-LOX3[3,38]. In mice missing either of these enzymes, reduced amounts of bound ceramides were observed, indicating that this process is essential for ceramide binding[4]. Furthermore, in essential fatty acid deficient pigs and mice, linoleic acid of EOCers became substituted with oleic acid, resulted in skin barrier dysfunction[11,39]. Thus, in FTMs the decreased amount of bound ceramides was likely due to the absence of sufficient amounts of linoleic acid esterified EOCers.

FTMs bound ceramides consisted predominately of MuCers and had a decreased chain length compared to those in *ex vivo* SC. Similar as to the bound ceramides, FTMs unbound ceramides also had an increased MuCer fraction and reduced chain length compared to *ex vivo* SC [21,25,40]. Hence, changes in FTMs bound ceramide composition were comparable to changes in the free ceramide fraction. It was observed that the LXR could alter the unbound SC lipid composition of FTMs [25]. Here, it was shown that the bound lipid composition improved upon LXR inhibition compared to the $FTM_{control}$, reducing the MuCers fraction and increasing the FTMs MCL. Contrastingly, an LXR agonist induced minor changes in the bound ceramide composition, expected as the endogenous substrate would be present in FTMs. Effects of LXR inhibition were comparable to the changes observed in the unbound lipid fraction upon LXR inhibition[25]. This showed that LXR has down-stream effects and can change the CLE composition.

In this study, bound glycosylated ceramides were observed in human *ex vivo* SC and also in tape-strips samples. Other reported that mice with a deficiency in sphingolipid activator proteins precursor ($pSAP^{-/-}$) and that in a Gaucher disease mouse model, the glycosylated bound ceramides were increased compared to wild type mice[41,42]. Yet, to our knowledge bound GlcCers had never been observed in

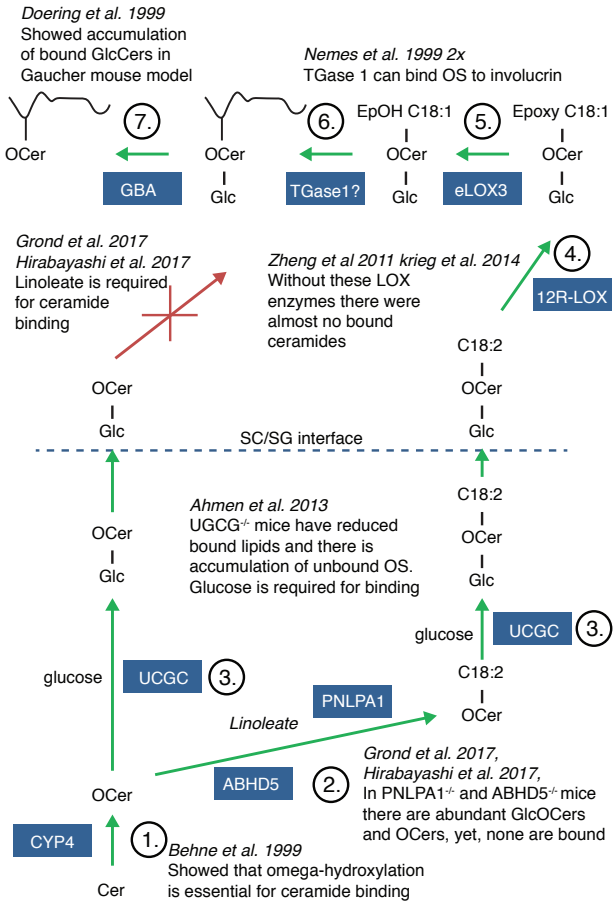

Figure 6.5: The pathway of ceramide binding.

1. Attachment of an omega-hydroxyl group. 2. Binding of a linoleate. 3. Binding of glucose. 4. Converting the linoleate to an epoxide. 5. Adding a hydroxyl group to the epoxide. 6. Binding of the ceramides. 7. Cleavage of the glucose group from the ceramide.

healthy human SC samples. The bound GlcCers in tape-stripped SC samples demonstrates that the bound GlcCers are also present in superficial layers of the SC, while GlcCers were not detected in the unbound lipids of tape-stripped samples. Free GlcCers primarily reside at the viable epidermis SC interface[14,43]. Whether the bound GlcCers escaped cleavage or that they have biological function is not known, yet, it does indicate that ceramide binding and glucosyl-cleavage are two separate processes. Previous studies showed that glycosylation was required for ceramide binding and free OS was not able to bind to the CE[18,44]. Furthermore, large amounts of bound glycosylated ceramides were observed when the glucosyl-cleavage capacity decreased[41,42]. Together with the present data, there is strong evidence that GlcCers are first bound to the CE followed by cleavage by glucosyl cerebrosidase (GBA1) to a bound ceramide[14].

Our data demonstrate selectivity in the binding process for ceramide linkage to the CE. Here, we propose a selective mechanism for ceramide binding based on our and previously published data (**Figure 6.5**). We propose the following: 1) Ω-hydroxylation of the acyl chain creating OCers[29]. 2) Mediated by PNLPA1 and with ABHD5 as a co-factor, a lineolate (C18:2) is bound to the OCers resulting in EOCer[18-20,45]. 3) By UDP-glucose ceramide glucosyltransferase (UCGC), glucose is attached to the remaining OCers and EOCers and both are stored in lamellar bodies. Glucose attachment is essential for ceramide binding[44]. GlcCers are released into the viable epidermis SC

interface. During this event, enzymes essential for ceramide binding colocalize[17]. In the next two steps (4, 5) 12R-LOX and eLOX3 convert the linoleate to a hydroxy-epoxide, yielding a ceramide with a hydroxy-epoxide and glucose attached. Literature reports that both modifications are necessary for ceramide binding, shown by PNLPA1 deficient mice which have abundant free OS and free Glc-OS in the SC, but virtually no bound ceramides[18]. 6) Transglutaminase 1 is hypothesized to bind the ceramides to the cornified envelope[46], but other mechanisms have not been excluded[47]. 7) GBA1 removes the glucose of the bound ceramide[14]. We show that this mechanism is selective towards MuCers and short chain ceramides, which further increases in FTMs. Yet, when the lipid synthesis is altered by LXR inhibition, compositional changes in the unbound ceramides were observed in the bound ceramides as well. This indicates that the ceramide binding is selective but still contingent on the lipid synthesis. Although it cannot be specified which part of the binding process is responsible for the selectivity, it can be deduced that it serves an important physiological function by providing flexibility to the corneocytes. Alterations in the binding and composition of the bound lipids could affect the formation of a proper SC lipid barrier.

Acknowledgements:

This work is part of the research Programme 12400 which is financed by the Netherlands Organization for Scientific Research (NWO).

References:

1 Rinnerthaler, M. *et al.* Age-related changes in the composition of the cornified envelope in human skin. *Exp Dermatol* **22**, 329-335 (2013).

2 Meguro, S., Arai, Y., Masukawa, Y., Uie, K. & Tokimitsu, I. Relationship between covalently bound ceramides and transepidermal water loss (TEWL). *Arch Dermatol Res* **292**, 463-468 (2000).

3 Munoz-Garcia, A., Thomas, C. P., Keeney, D. S., Zheng, Y. & Brash, A. R. The importance of the lipoxygenase-hepoxilin pathway in the mammalian epidermal barrier. *Biochimica et biophysica acta* **1841**, 401-408 (2014).

4 Krieg, P. *et al.* Aloxe3 knockout mice reveal a function of epidermal lipoxygenase-3 as hepoxilin synthase and its pivotal role in barrier formation. *The Journal of investigative dermatology* **133**, 172-180 (2013).

5 Wertz, P. W., Madison, K. C. & Downing, D. T. Covalently bound lipids of human stratum corneum. *The Journal of investigative dermatology* **92**, 109-111 (1989).

6 Hill, J., Paslin, D. & Wertz, P. W. A new covalently bound ceramide from human stratum corneum -omega-hydroxyacylphytosphingosine. *Int J Cosmet Sci* **28**, 225-230 (2006).

7 Farwanah, H. *et al.* Separation and mass spectrometric characterization of covalently bound skin ceramides using LC/APCI-MS and Nano-ESI-MS/MS. *Journal of chromatography. B, Analytical technologies in the biomedical and life sciences* **852**, 562-570 (2007).

8 Motta, S. *et al.* Ceramide composition of the psoriatic scale. *Biochimica et biophysica acta* **1182**, 147-151 (1993).

9 Stewart, M. E. & Downing, D. T. The omega-hydroxyceramides of pig epidermis are attached to corneocytes solely through omega-hydroxyl groups. *Journal of lipid research* **42**, 1105-1110 (2001).

10 Marekov, L. N. & Steinert, P. M. Ceramides are bound to structural proteins of the human foreskin epidermal cornified cell envelope. *J Biol Chem* **273**, 17763-17770 (1998).

11 Elias, P. M. *et al.* Formation and functions of the corneocyte lipid envelope (CLE). *Biochimica et biophysica acta* **1841**, 314-318 (2014).

12 Matsui, T. & Amagai, M. Dissecting the formation, structure and barrier function of the stratum corneum. *Int Immunol* **27**, 269-280 (2015).

13 Feingold, K. R. & Elias, P. M. Role of lipids in the formation and maintenance of the cutaneous permeability barrier. *Biochimica et biophysica acta* **1841**, 280-294 (2014).

14 van Smeden, J. *et al.* In situ visualization of glucocerebrosidase in human skin tissue: zymography versus activity-based probe labeling. *Journal of lipid research* **58**, 2299-2309 (2017).

15 Kalinin, A. E., Kajava, A. V. & Steinert, P. M. Epithelial barrier function: assembly and structural features of the cornified cell envelope. *Bioessays* **24**, 789-800 (2002).

16 Eckhart, L., Lippens, S., Tschachler, E. & Declercq, W. Cell death by cornification. *Biochimica et biophysica acta* **1833**, 3471-3480 (2013).

17 Li, H., Lorie, E. P., Fischer, J., Vahlquist, A. & Torma, H. The expression of epidermal lipoxygenases and transglutaminase-1 is perturbed by NIPAL4 mutations: indications of a common metabolic pathway essential for skin barrier homeostasis. *The Journal of investigative dermatology* **132**, 2368-2375 (2012).

18 Grond, S. *et al.* PNPLA1 Deficiency in Mice and Humans Leads to a Defect in the Synthesis of Omega-O-Acylceramides. *The Journal of investigative dermatology* **137**, 394-402 (2017).

19 Grond, S. *et al.* Skin Barrier Development Depends on CGI-58 Protein Expression during Late-Stage Keratinocyte Differentiation. *The Journal of investigative dermatology* **137**, 403-413 (2017).

20 Hirabayashi, T. *et al.* PNPLA1 has a crucial role in skin barrier function by directing acylceramide biosynthesis. *Nat Commun* **8**, 14609 (2017).

21 Mieremet, A., Rietveld, M., van Dijk, R., Bouwstra, J. A. & El Ghalbzouri, A. Recapitulation of Native Dermal Tissue in a Full-Thickness Human Skin Model Using Human Collagens. *Tissue Eng Part A* **24**, 873-881 (2018).

22 Thakoersing, V. S. *et al.* Unraveling barrier properties of three different in-house human skin equivalents. *Tissue Eng Part C Methods* **18**, 1-11 (2012).

23 Schmuth, M., Moosbrugger-Martinz, V., Blunder, S. & Dubrac, S. Role of PPAR, LXR, and PXR in epidermal homeostasis and inflammation. *Biochimica et biophysica acta* **1841**, 463-473 (2014).

24 Griffett, K. & Burris, T. P. Promiscuous activity of the LXR antagonist GSK2033 in a mouse model of fatty liver disease. *Biochem Biophys Res Commun* **479**, 424-428 (2016).

25 Helder, R. W. J. *et al.* Improved lipid composition in human skin equivalents after liver-X-receptor deactivation. *Journal of investigative dermatology*.

26 Boiten, W., Absalah, S., Vreeken, R., Bouwstra, J. & van Smeden, J. Quantitative analysis of ceramides using a novel lipidomics approach with three dimensional response modelling. *Biochimica et biophysica acta* **1861**, 1652-1661 (2016).

27 t'Kindt, R. *et al.* Profiling and characterizing skin ceramides using reversed-phase liquid chromatography-quadrupole time-of-flight mass spectrometry. *Analytical chemistry* **84**, 403-411 (2012).

28 Rabionet, M., Gorgas, K. & Sandhoff, R. Ceramide synthesis in the epidermis. *Biochimica et biophysica acta* **1841**, 422-434 (2014).

29 Behne, M. *et al.* Omega-hydroxyceramides are required for corneocyte lipid envelope (CLE) formation and normal epidermal permeability barrier function. *The Journal of investigative dermatology* **114**, 185-192 (2000).

30 Uchida, Y. & Holleran, W. M. Omega-O-acylceramide, a lipid essential for mammalian survival. *J Dermatol Sci* **51**, 77-87 (2008).
31 Beard, J. D., Guy, R. H. & Gordeev, S. N. Mechanical tomography of human corneocytes with a nanoneedle. *The Journal of investigative dermatology* **133**, 1565-1571 (2013).
32 Milani, P., Chlasta, J., Abdayem, R., Kezic, S. & Haftek, M. Changes in nano-mechanical properties of human epidermal cornified cells depending on their proximity to the skin surface. *J Mol Recognit*, e2722 (2018).
33 Bouwstra, J. A. *et al.* Water distribution and related morphology in human stratum corneum at different hydration levels. *The Journal of investigative dermatology* **120**, 750-758 (2003).
34 Mojumdar, E. H., Kariman, Z., van Kerckhove, L., Gooris, G. S. & Bouwstra, J. A. The role of ceramide chain length distribution on the barrier properties of the skin lipid membranes. *Biochim Biophys Acta* **1838**, 2473-2483 (2014).
35 Paloncyova, M. *et al.* Structural Changes in Ceramide Bilayers Rationalize Increased Permeation through Stratum Corneum Models with Shorter Acyl Tails. *J Phys Chem B* **119**, 9811-9819 (2015).
36 Ponec, M., Boelsma, E. & Weerheim, A. Covalently bound lipids in reconstructed human epithelia. *Acta Derm Venereol* **80**, 89-93 (2000).
37 Ponec, M., Weerheim, A., Lankhorst, P. & Wertz, P. New acylceramide in native and reconstructed epidermis. *The Journal of investigative dermatology* **120**, 581-588 (2003).
38 Zheng, Y. *et al.* Lipoxygenases mediate the effect of essential fatty acid in skin barrier formation: a proposed role in releasing omega-hydroxyceramide for construction of the corneocyte lipid envelope. *J Biol Chem* **286**, 24046-24056 (2011).
39 Melton, J. L., Wertz, P. W., Swartzendruber, D. C. & Downing, D. T. Effects of essential fatty acid deficiency on epidermal O-acylsphingolipids and transepidermal water loss in young pigs. *Biochimica et biophysica acta* **921**, 191-197 (1987).
40 Thakoersing, V. S. *et al.* Increased presence of monounsaturated fatty acids in the stratum corneum of human skin equivalents. *The Journal of investigative dermatology* **133**, 59-67 (2013).
41 Doering, T. *et al.* Sphingolipid activator proteins are required for epidermal permeability barrier formation. *J Biol Chem* **274**, 11038-11045 (1999).
42 Doering, T., Proia, R. L. & Sandhoff, K. Accumulation of protein-bound epidermal glucosylceramides in beta-glucocerebrosidase deficient type 2 Gaucher mice. *FEBS Lett* **447**, 167-170 (1999).
43 Hamanaka, S. *et al.* Human epidermal glucosylceramides are major precursors of stratum corneum ceramides. *The Journal of investigative dermatology* **119**, 416-423 (2002).
44 Amen, N. *et al.* Differentiation of epidermal keratinocytes is dependent on glucosylceramide:ceramide processing. *Hum Mol Genet* **22**, 4164-4179 (2013).
45 Pichery, M. *et al.* PNPLA1 defects in patients with autosomal recessive congenital ichthyosis and KO mice sustain PNPLA1 irreplaceable function in epidermal omega-O-acylceramide synthesis and skin permeability barrier. *Hum Mol Genet* **26**, 1787-1800 (2017).
46 Nemes, Z., Marekov, L. N., Fesus, L. & Steinert, P. M. A novel function for transglutaminase 1: attachment of long-chain omega-hydroxyceramides to involucrin by ester bond formation. *Proc Natl Acad Sci U S A* **96**, 8402-8407 (1999).
47 Elias, P. M. *et al.* Basis for the permeability barrier abnormality in lamellar ichthyosis. *Exp Dermatol* **11**, 248-256 (2002).

6 Supplementals chapter 6

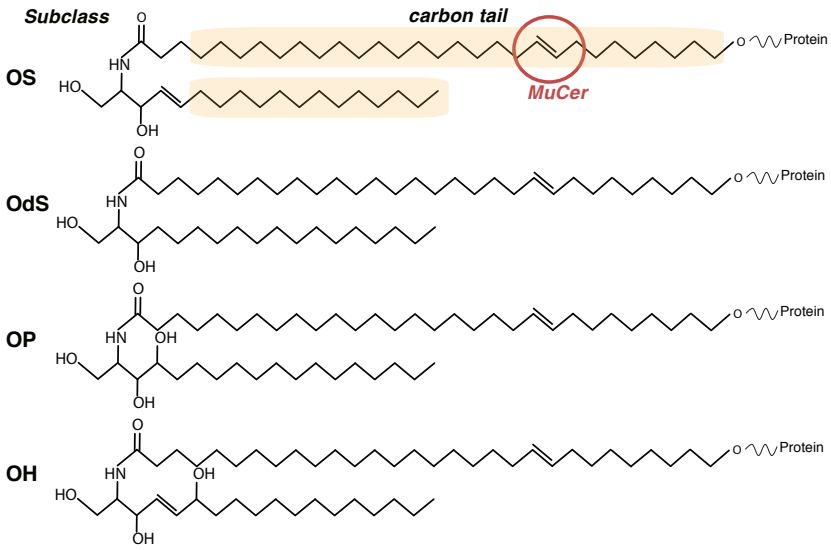

Supplemental S6.1: Bound ceramide structures

Ceramides standard used for the quantification of the ceramides and structures of the bound ceramide subclasses. The first one has the, carbon tail, and unsaturation indicated.

Supplemental S6.2: Synthetic ceramides that were used as calibrators for LC/MS analysis.

Numbers in brackets indicate the number of carbon atoms in the fatty acid chain and sphingosine chain, respectively.

Ceramides		
N(24)dS(18) [1]	N(16)S(18) [1]	E(18:2)O(30)S(18) [2]
N(18)dS(18) [1]	N(24)P(18) [2]	E(18:2)O(27)S(18) [2]
N(16)dS(18) [1]	N(16)P(18) [2]	E(18:2)O(30)P(S18) [2]
N(24)S(18) [2]	A(24)S(18) [1]	E(18:2)O(27)P(18) [2]
N(22)S(18) [1]	A(22)S(18) [1]	N(24deu)S(18) [23]
N(20)S(18) [1]	A(16)S(18) [1]	
N(18)S(18) [1]	A(24)P(18) [1]	

[1] Avanti polar lipids (Alabaster, USA) [2] Evonik Industries (Essen, Germany) [3]ISTD

Supplemental S6.3: Extraction effiency and Recovery

To determine the extraction efficiency, four sheets of ex vivo SC from two donors (two sheets per donor) were used. First, the unbound lipids were extracted and the SC washed with chloroform (as described in the methods). Then, two consecutive bound lipid extractions were performed on the SC sheets. To compare both extracts, the first extract was dissolved in 1.4 ml and the second in 0.28 ml. A fifth of the volume was chosen as it was expected that the second extract would only contain a limited amount of ceramides. The samples were measured and the ceramides that could be detected in the second extracted used to determine the extraction efficiency. **Supplemental S6.3 Table I** shows the percentage of these ceramides that was detected in the first bound lipid extract.

Supplemental S6.3 Table1:

The extraction efficiency as the percentage in the first extract compared to the total of two consecutive saponifications. Values were calculated for each ceramide per SC sample. All value is the summed detection of the listed ceramides. The mean per ceramide, per sample and total mean are given as well.

Extraction Efficiency %	Donor 1		Donor 2		Mean
Ceramide	Sample 1	Sample 2	Sample 1	Sample 2	
OdS C58	69.5	100.0	100.0	100.0	92.4
OdS C56	83.1	100.0	91.5	100.0	93.7
OS C52	98.0	99.2	99.4	99.5	99.0
OS C51	98.2	99.2	100.0	100.0	99.4
OS C50	98.5	99.3	99.5	99.6	99.2
OS C48	98.4	100.0	100.0	100.0	99.6
OP C52	97.8	100.0	100.0	100.0	99.5
OH C52	98.9	99.4	100.0	100.0	99.6
OH C50	99.0	99.6	99.7	99.8	99.5
OH C48	98.6	99.5	100.0	99.8	99.5
All	98.3	99.4	99.7	99.8	99.3
Mean	94.0	99.6	99.0	99.9	98.1

To determine the recovery of the bound lipid extraction, 3 mixtures of the calibration standards (listed in **Supplemental S6.2**) were aliquoted into two 1 ml samples of 2 µM. One aliquot was extracted by saponification and the other was left untreated. Both were analyzed and the recovery was determined as the difference in detection between the extracted and non-extracted sample relative to the detection in the non-extracted samples. **Supplemental S6.3 Table 2** depicts the recovery as percentage.

Supplemental S6.3 Table 2:

Recovery of the bound lipid extraction, as percentage remaining after extraction compared to a non-extracted sample. The mean of all three samples per ceramide and the total mean are given.

Recovery % Ceramide	**sample 1**	**sample 2**	**sample 3**	**mean**
NdS C42	105.1	88.0	95.9	96.3
NdS C36	99.1	88.5	94.2	93.9
NdS C34	101.0	83.3	98.5	94.3
NS C42	99.7	93.3	90.1	94.4
NS C40	103.5	83.3	87.2	91.3
NS C38	95.6	87.5	93.8	92.3
NS C36	103.1	89.9	98.0	97.0
NS C34	113.2	92.6	95.5	100.5
NP C42	99.6	81.0	89.7	90.1
NP C34	97.5	90.9	105.6	98.0
AS C42	105.2	82.1	92.0	93.1
AS C40	103.8	77.9	93.6	91.8
AS C34	96.3	88.6	93.7	92.9
AP C42	90.5	80.5	94.6	88.5
			mean	93.9

Supplemental S6.4 Overview of observed fragments from multiple OdS Ceramides

	Ceramide	**OdS C56**	**OdS C56**	**OdS C56:1**	**OdS C56:1**
	Chem Form.	$C_{56}H_{113}O_4NH$	$C_{56}H_{113}O_4NH$	$C_{56}H_{111}O_4NH$	$C_{56}H_{111}O_4NH$
	Select mass.	864.87478	864.87478	862.85913	862.85913
	Col (eV)	50	40	50	40
Frag. (m/z)	Chain sph	C22-26	C22-26	C22-26	C20-26
294.3	C20				x
308.3	C21				
322.3	C22	x	x	x	x
336.3	C23				
350.3	C24	x	x	x	x
364.3	C25		x		
378.3	C26	x	x		x
	+18				
312.3	C20				x
326.3	C21				
340.3	C22			x	x
354.3	C23				
368.3	C24	x	x	x	x
382.3	C25		x		
396.3	C26	x	x	x	x
	+2*18				
358.3	C22				-
372.3	C23				
386.3	C24	x	x		x
400.3	C25				
414.3	C26	x	x		x
	-CH2OH				
338	C24		x	x	
352	C25				
366	C26	x	x		

Table S6.4 continued

	Ceramide	**OdS C52**	**OdS C52**	**OdS C52:1**	**OdS C52:1**
	Chem Form.	$C_{52}H_{105}O_4NH$	$C_{52}H_{105}O_4NH$	$C_{52}H_{103}O_4NH$	$C_{52}H_{103}O_4NH$
	Select mass.	808.81218	808.81218	806.79653	806.79653
	Col (eV)	50	40	50	40
Frag. (m/z)	Chain sph	C18-24	C20-24	C18-24	C18-24
266.3	C18	x		x	x
280.3	C19				
294.3	C20	x	x	x	x
308.3	C21	x			
322.3	C22	x	x	x	x
	+18				
284.3	C18			x	x
298.3	C19	x			
312.3	C20	x	x	x	x
326.3	C21	x			
340.3	C22	x	x		x
354.3	C23				
368.3	C24	x	x		
	+2*18				
274.3	C16				
330.3	C20		x		
344.3	C21				
358.3	C22		x		
	-CH2OH				
254	C18	x		x	
268	C19	x			
282	C20	x	x	x	x
296	C21	x			
310	C22	x	x	x	
324	C23				
338	C24			x	x

	Ceramide	**OdS C51**	**OdS C51**	**OdS C50**	**OdS C50**
	Chem Form.	$C_{51}H_{103}O_4NH$	$C_{51}H_{103}O_4NH$	$C_{50}H_{101}O_4NH$	$C_{50}H_{101}O_4NH$
	Select mass.	794.79653	794.79653	780.78088	780.78088
	Col (eV)	50	40	50	40
Frag.(m/z)	Chain sph	C17-23	C18-22	18-20	18-22
266.3	C18			x	x
280.3	C19	x		x	
294.3	C20	x	x	x	x
308.3	C21	x	x		
322.3	C22	x	x		x
336.3	C23	x			
	+18				
270.3	C17	x			
284.3	C18	x	x	x	x
298.3	C19	x	x		x
312.3	C20	x	x	x	x
326.3	C21	x	x		x
340.3	C22	x	x		x
	+2*18				
302.3	C18				x
316.3	C19		x		
330.3	C20				x
344.3	C21		x		
	-CH2OH				
240	C17	x			
254	C18	x		x	x
268	C19	x		x	
282	C20	x		x	x
296	C21	x			

Supplemental S6.5

To determine if the process of saponification with a subsequent Bligh and Dyer extraction, will extract unintended material a blank extraction was performed. Three saponification procedures were performed in empty vails. The extraction solvent mixtures were added to the neutralized solvents and the Bligh and Dyer extraction as described in the method section. The obtained organic phases were evaporated and reconstituted in 1.5 ml of chloroform:methanol (2:1). Using the gravimetric approached the dry weight and subsequent concentration of material in the extracts was determined. Supplemental table 3 depicts the concentration of these samples. This showed there was a substantial amount of material extracted. This material is probably NaCl which is produced during the neutralization of the saponification. Although the solvent are chloroform and methanol, these are able to dissolve a fraction of water and salt. Therefore, the lipid concentration of saponified samples could not be determined.

Supplemental S6.5 Table 1: *concentration of blank extracts*

	Concentration mg/ml
Sample 1	0.155
Sample 2	0.151
Sample 3	0.113

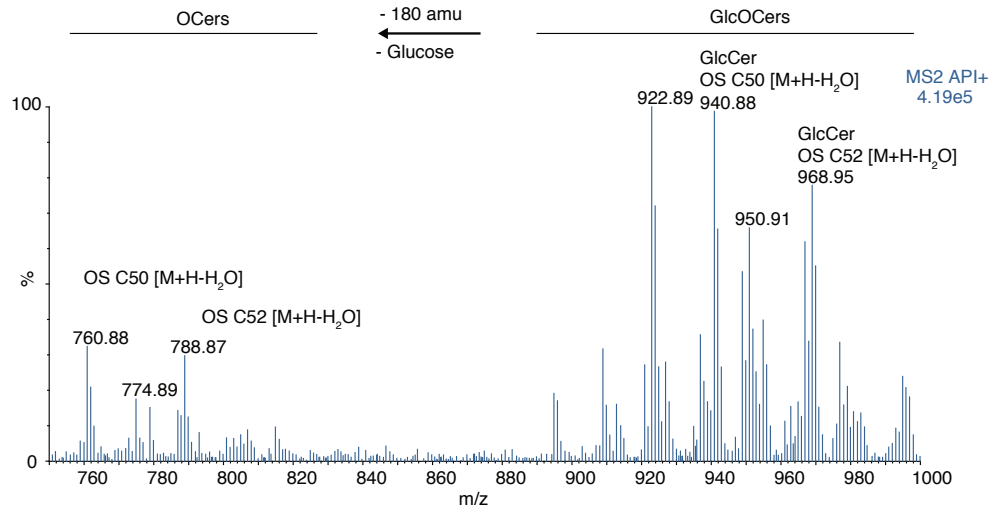

Supplemental S6.6

A smoothed and centered spectrum of the bound glucosylceramide eluting at an Rt of 9.8 min. The m/z of O-GluCers and the m/z of the corresponding OCer were observed at the same Rt. These could be distinguished by a difference of 180 amu (the mass of a glucose).

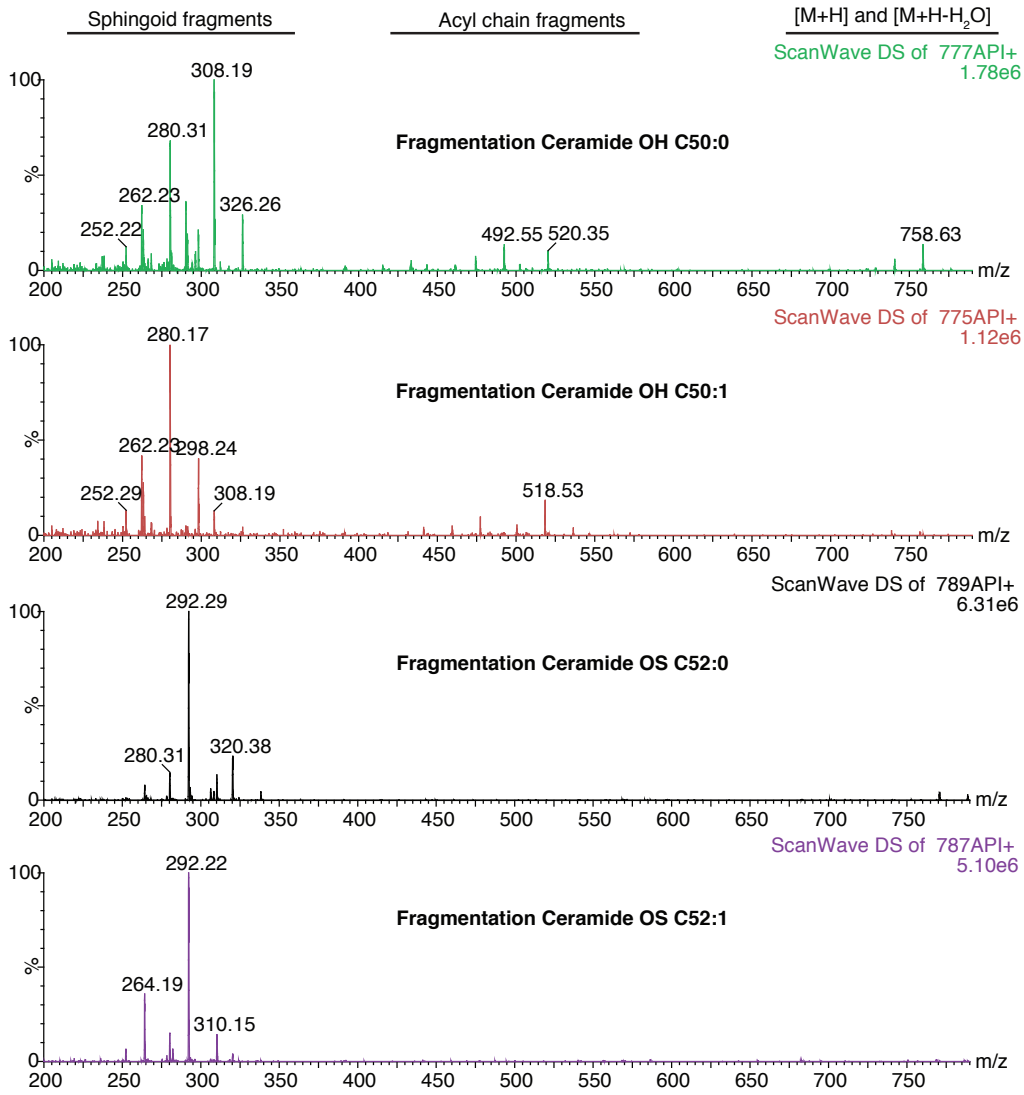

Supplemental S6.7: Saturated sphingoid chains in bound MuCers

The figure shows unsmoothed fragmentation spectra of both the saturated and unsaturated ceramide of the same subclass with the same total chain length. This is shown for two ceramide of different subclasses. Fragmentation was performed on extracted bound ceramides from ex vivo SC. The same sphingoid fragments were observed in both the saturated and unsaturated ceramide, observe as the same mass (exemplified by m/z 308.19 and 292.22). This showed that the unsaturation was in the acyl chain of the ceramides. As conformation the unsaturated acyl chain was observed in the OH ceramides (520.35 compared to 518.53).

	SC Donor 1		SC Donor 2		SC Donor 3	
Subclass	Molar%	SD	Molar%	SD	Molar%	SD
NdS	2.23	0.44	2.77	1.24	3.39	1.01
NS	0.76	0.11	0.66	1.15	1.22	1.07
NP	0.44	0.33	0.82	0.69	1.11	0.55
NH	1.52	0.17	1.38	0.43	1.60	0.46
AP	1.06	0.34	1.61	0.22	1.72	0.22
AH	1.12	0.17	1.18	0.16	1.23	0.12
EOdS	14.53	1.04	12.41	7.25	16.41	7.24
EOS	10.59	1.11	9.46	2.09	10.91	2.54
EOP	7.06	1.21	5.11	4.23	7.65	4.00
EOH	6.46	0.65	5.59	2.03	6.93	2.17
OdS	41.61	5.44	36.04	7.10	39.86	1.93
OS	8.87	2.19	2.82	11.01	7.85	13.08
OP	14.62	4.10	8.86	9.76	14.77	9.71
OH	12.34	2.10	8.09	10.44	13.77	10.50

Supplemental S6.8: MuCer percentage per subclass in unbound SC lipids

Table depicts the average molar percentage and SD (n=3) of MuCers within a subclass. The total amount in moles of both saturated and unsaturated ceramides of a subclass is set as a 100%. This is shown for 3 different SC donors.

Supplemental S6.9

A linear mixed model was made to compare the percentage of MuCers between bound ceramides and the unbound taking into count the differences between subclasses. The bound ceramide was set as the control condition of which the intercept (mean) is given. The effects size indicates the change in value due to the change in examined group (unbound OCers or EOCers). The p-value indicates the probability that the intercept or effect size is non-zero.

	MuCer % per subclass	OdS/EOdS		95% Confidence Interval		OS/EOS		95% Confidence Interval	
		Size	p-value	lower	upper	Size	p-value	lower	upper
	Intercept (bound)	37.62	0.008	21.77	53.47	22.25	0.024	6.40	38.10
Effect size	Unbound EOCers	-20.30	<0.001	-23.43	-17.17	-10.98	<0.001	-14.11	-7.85
	Unbound OCers	3.50	0.029	0.37	6.64	-10.90	<0.001	-14.04	-7.77

		OP/EOP		95% Confidence Interval		OH/EOH		95% Confidence Interval	
		Size	p-value	lower	upper	Size	p-value	lower	upper
	Intercept (bound)	37.02	0.008	21.17	52.87	27.24	0.016	11.39	43.09
Effect size	Unbound EOCers	-28.90	<0.001	-32.03	-25.77	-20.15	<0.001	-23.29	-17.02
	Unbound OCers	-21.05	<0.001	-24.18	-17.92	-11.79	<0.001	-14.92	-8.66

SPSS code used to obtain the result of the model. The code was ran separately for each subclass.

```
MIXED MuPr[1] BY Condition[2] Subclass
 /CRITERIA=CIN(95) MXITER(100) MXSTEP(10) SCORING(1) SINGULAR(0.000000000001) HCONVERGE(0,
   ABSOLUTE) LCONVERGE(0, ABSOLUTE) PCONVERGE(0.000001, ABSOLUTE)
 /FIXED=Condition Subclass Condition*Subclass | SSTYPE(3)
 /METHOD=REML
 /PRINT=SOLUTION TESTCOV
 /RANDOM=INTERCEPT | SUBJECT(SC) COVTYPE(VC)
          /EMMEANS=TABLES(Condition*Subclass) .
```

[1]MuPr = the MuCer percentage per subclass
[2]Condition = Bound, Unbound Ocers, and EOcers

Supplemental S6.10

A linear mixed model was made to compare the MCL between bound ceramides and the unbound ceramides taking into account if these were saturated or desaturated. The bound ceramides were set as the control condition of which the intercept (mean) is given. The effects size indicates the change in value due to the change in examined group (unbound OCer, EOCer -18 carbons, or if it was unsaturated). The interaction shows the additional change when two different condition occur together additional to the changes of both independent conditions. In other words the MCL of unsaturated unbound OCer was more than 2.08 carbons longer than the saturated unbound OCer. The p-value indicates the probability that the intercept, effect size or interaction is non-zero.

	MCL (Carbon atoms)			95% Confidence Interval	
		Estimate	p-value	lower	upper
	Intercept (bound)	50.18	<0.01	49.95	50.41
Effect sizes	Unbound OCers	0.66	<0.001	0.43	0.88
	EOCers	0.77	<0.001	0.55	1.00
	Unsaturated	2.08	<0.001	1.85	2.30
Interaction	Unbound OCers * Unsaturated	0.93	<0.001	0.61	1.25
	Unbound EOCers *Unsaturated	1.41	<0.001	1.09	1.73

SPSS code used to make this model

```
MIXED MCL BY Condition[1] saturation
 /CRITERIA=CIN(95) MXITER(100) MXSTEP(10) SCORING(1) SINGULAR(0.000000000001)
HCONVERGE(0,
   ABSOLUTE) LCONVERGE(0, ABSOLUTE) PCONVERGE(0.000001, ABSOLUTE)
 /FIXED=Condition saturation Condition*saturation | SSTYPE(3)
 /METHOD=REML
 /PRINT=SOLUTION TESTCOV
 /RANDOM=INTERCEPT | SUBJECT(SC) COVTYPE(VC)
 /EMMEANS=TABLES(Condition*saturation).
```

[1]Condition = bound, unbound Ocer, EOcer -18 carbon

Supplemental S6.11: Output of linear mixed models of FTMs with LXR agonist and antagonist.

Output of the linear mixed model comparing the bound ceramides in Ex Vivo$_{control}$, FTM$_{Control,}$ FTM$_{DMSO,}$ FTM$_{AGONST}$, and FTM$_{AGONIST}$. For these models only the output for FTM$_{DMSO}$ compared to FTM$_{Control}$ is depicted. The models were ran multiple times with different groups set as intercept: Ex vivo$_{control}$, FTM$_{Control}$, and FTM$_{agonist}$. Using these 3 runs all groups could be compared.

Supplemental S6.11 Table 1: Comparison of total bound ceramide amount and MuCer percentage.

		Amount ceramides µg/ mg SC		**95% Confidence Interval**		**MuCer**		**95% Confidence Interval**	
		Size	p-value	lower	upper	Size	p-value	lower	upper
	Intercept (Ex vivo)	7.058	<0.001	5.277	8.840	25.08	0.001	16.26	33.90
Effect size	FTM control	-5.394	0.002	-7.858	-2.929	61.26	<0.001	48.86	73.66
	FTM agonist	-5.483	0.002	-7.948	-3.018	62.26	<0.001	49.86	74.66
	FTM antagonist	-5.511	0.002	-7.976	-3.046	46.22	<0.001	33.82	58.62

Table S6.11.tabel1 continued

		Amount ceramides µg/ mg SC		95% Confidence Interval		MuCer		95% Confidence Interval	
		Size	p-value	lower	upper	Size	p-value	lower	upper
	Intercept (FTM control)	1.664	0.060	-0.097	3.425	86.33	<0.001	77.61	95.06
	FTM DMSO	0.698	0.368	-0.938	2.334	-1.82	0.197	-4.73	1.09
Effect size	FTM agonist	-0.089	0.893	-1.517	1.338	1.00	0.402	-1.52	3.52
	FTM antagonist	-0.117	0.860	-1.545	1.311	-15.03	<0.001	-17.56	-12.51

		Amount ceramides µg/ mg SC		95% Confidence Interval		MuCer		95% Confidence Interval	
		Size	p-value	lower	upper	Size	p-value	lower	upper
	Intercept (FTM agonist)	1.575	0.072	-0.186	3.336	87.33	<0.001	78.61	96.06
Effect size	FTM antagonist	-0.028	0.967	-1.456	1.400	-16.03	<0.001	-18.56	-13.51

Supplemental S6.11 Table 2: Comparison of total bound mean chain length saturated and unsaturated

		MCL Sat		95% Confidence Interval		MCL unSat		95% Confidence Interval	
		Size	p-value	lower	upper	Size	p-value	lower	upper
	Intercept (Ex vivo)	50.18	<0.001	49.90	50.46	52.32	<0.001	52.04	52.60
	FTM control	-0.31	0.113	-0.71	0.09	-1.45	<0.001	-1.85	-1.05
Effect size	FTM agonist	-0.67	0.005	-1.07	-0.27	-2.14	<0.001	-2.54	-1.74
	FTM antagonist	0.09	0.612	-0.31	0.49	-0.26	0.170	-0.66	0.14

		MCL Sat		95% Confidence Interval		MCL unSat		95% Confidence Interval	
		Size	p-value	lower	upper	Size	p-value	lower	upper
	Intercept (FTM control)	49.87	<0.001	49.58	50.17	50.87	0.000	50.58	51.16
	FTM DMSO	0.12	0.406	-0.18	0.43	0.00	0.989	-0.31	0.30
Effect size	FTM agonist	-0.36	0.011	-0.62	-0.09	-0.69	<0.001	-0.96	-0.42
	FTM antagonist	0.40	0.005	0.13	0.67	1.19	<0.001	0.92	1.46

		MCL Sat		95% Confidence Interval		MCL unSat		95% Confidence Interval	
		Size	p-value	lower	upper	Size	p-value	lower	upper
	Intercept (FTM agonist)	49.52	<0.001	49.22	49.81	50.18	<0.001	49.89	50.47
Effect size	FTM antagonist	0.76	<0.001	0.49	1.02	1.88	<0.001	1.61	2.15

SPSS code used to make the models of supplemtenal S6.11

```
MIXED Total BY Group
  /CRITERIA=CIN(95) MXITER(100) MXSTEP(10) SCORING(1) SINGULAR(0.000000000001)
HCONVERGE(0,
   ABSOLUTE) LCONVERGE(0, ABSOLUTE) PCONVERGE(0.000001, ABSOLUTE)
 /FIXED=Group | SSTYPE(3)
 /METHOD=REML
 /PRINT=SOLUTION TESTCOV
 /RANDOM=INTERCEPT | SUBJECT(Don) COVTYPE(VC).
```

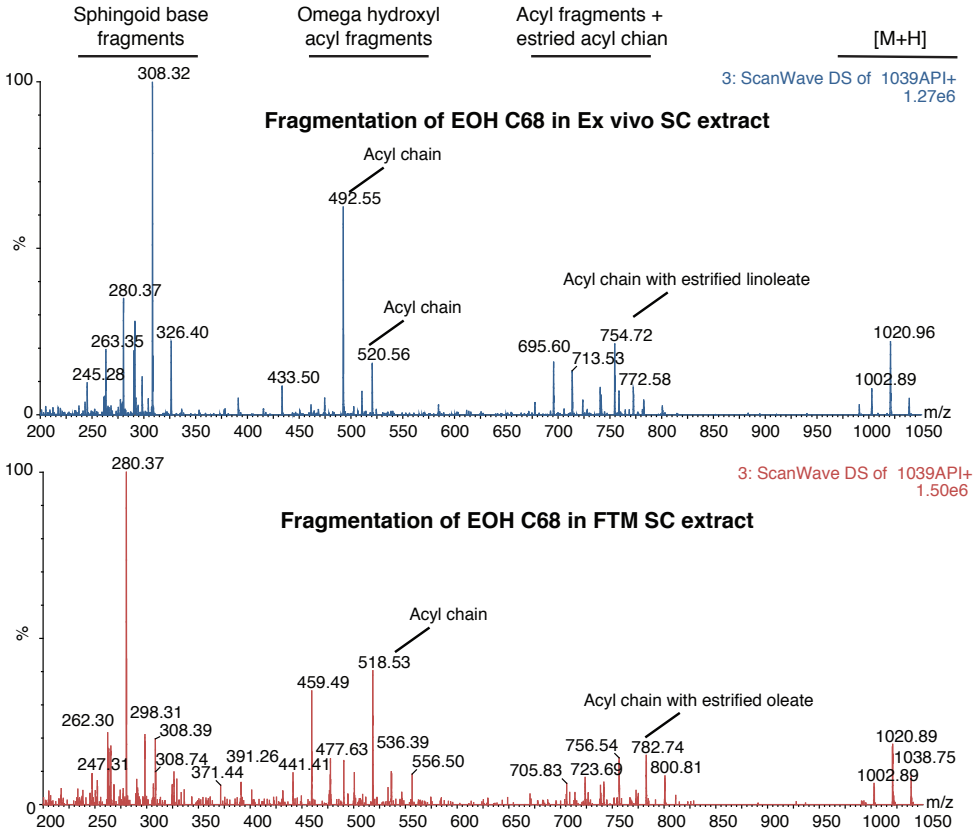

Supplemental S6.12: Oleic acid instead of linoleic acid attached as acyl chain in EOCers.

Fragmentation of EOH C68 (1039 amu) at 40 eV in ex vivo and FTM SC lipid extracts. The characteristic fragments are indicated above the figures. The fragments of both a saturated and unsaturated acyl chain are indicated (also present in supplemental S6.8). The fragments with the linoleate and oleate attached to it are indicated as well.